

## Double intertropical convergence zones—a new look using scatterometer

W. Timothy Liu and Xiaosu Xie

Jet Propulsion Laboratory, California Institute of Technology, Pasadena, CA, USA

Received 4 May 2002; revised 3 June 2002; accepted 20 June 2002; published 29 November 2002.

[1] The high-resolution wind vectors observed by the space-based scatterometer QuikSCAT, from 1999 to 2002, show that the double intertropical convergence zones (ITCZ) exist in the Atlantic and the eastern Pacific oceans for most of the annual cycle, and are far more extensive than previously recognized. For most of the time, the southern ITCZ is weaker than the northern one. The stronger ITCZ occurs when the northerly trade winds meet the southerly trade winds over warm water, resulting in deep convection. The weaker ITCZ over cooler water is caused by the deceleration of the surface winds as they approach the cold upwelling water near the equator. Decreases in vertical mixing and increases in vertical wind shear in the atmospheric boundary layer are suggested to be the causes of the deceleration of the trade winds as they move from warmer to colder water. *INDEX TERMS:* 1640 Global Change: Remote sensing; 4504 Oceanography: Physical: Air/sea interactions (0312); 4247 Oceanography: General: Marine meteorology; 4231 Oceanography: General: Equatorial oceanography. *Citation:* Liu, W. T., and X. Xie, Double intertropical convergence zones—a new look using scatterometer, *Geophys. Res. Lett.*, 29(22), 2072, doi:10.1029/2002GL015431, 2002.

### 1. Introduction

[2] The intertropical convergence zone (ITCZ) is defined as the narrow and zonally-oriented belt of surface wind convergence located north of the equator in the Atlantic and eastern Pacific oceans. The ITCZ is believed to be driving the Hadley circulation. Its annual meridional migration and its interannual variations have been well studied, largely through satellite cloud images and inferred precipitation, as the manifestation of deep convection. Through similar satellite images, a parallel intertropical convergence zone south of the equator (SITCZ) in the eastern Pacific Ocean has been identified, to form the double ITCZ. Convergence areas are also found near the equator in the western Pacific and Indian Oceans, but they are rather diffused and will not be discussed in this study.

[3] Since *Hubert et al.* [1969] asked the rhetorical question of whether the double ITCZ is fact or fiction, the existence, location, and seasonality of the double ITCZ remain controversial after more than thirty years. *Hubert et al.* [1969], using cloud brightness temperature measured by space-based radiometer, showed only transient SITCZ in the boreal spring in the Pacific, and concluded that double ITCZ is not a characteristic feature of tropical circulation. *Waliser and Gautier* [1993], *Zhang* [2001], and *Lietzke et*

*al.* [2001] also found SITCZ during boreal spring in the eastern Pacific, using highly reflective clouds, rainfall distribution, and satellite moisture soundings, respectively.

[4] By definition, ITCZ should be examined through surface wind convergence, but surface wind convergence is generally not computed because of the poor resolution of wind maps derived from ship reports. The first study of SITCZ, using three years of space-based wind vectors from the scatterometer on the first European Remote Sensing satellite (ERS-1), is by *Zheng et al.* [1997]. Besides examining the ITCZ north of the equator, they also pointed out the SITCZ in the eastern Pacific during boreal spring. *Halpern and Hung* [2001], using nine years of ERS data, identified the South Pacific ITCZ in March-April, with threshold convergence collocated with threshold sea surface temperature (SST). Using the higher resolution QuikSCAT winds, *Grodsky and Carton* [2001] and *Liu* [2002] recently revealed a SITCZ in the western Atlantic in boreal summers.

[5] In this study, QuikSCAT data will be used to show that the double ITCZ is much more extensive, with parallel convergence zones of varying strength year-round. The difference in the mechanisms that sustain the two types of wind convergence will be postulated. Weak wind convergence may not have the same manifestation in clouds and precipitation as strong wind convergence, but will have impacts in both atmospheric and ocean circulations.

### 2. Past Hypothesis

[6] Most of the investigators attempted to relate the existence and location of SITCZ to SST distribution through the pressure gradient hypothesis of *Lindzen and Nigam* [1987]. *Lietzke et al* [2001], *Halpern and Hung* [2001], and others postulated that the stronger SST gradient between the SITCZ and the equatorial cold tongue during boreal springs in the eastern Pacific creates sufficient pressure gradient in the atmosphere and causes a southward flow from the equator which converges at the SITCZ with northward winds from the cooler southern oceans. If such a conceptual model is valid, one expects that the SITCZ would collocate with the maximum local SST, and that winds will blow both northward and southward from the equator to feed both convergence zones. QuikSCAT data do not support such inferences.

### 3. Data

[7] The surface wind vectors are derived from observations of the radar scatterometer - QuikSCAT. QuikSCAT measures surface wind speed and direction, covering 93%

of the global ocean under clear and cloudy conditions, night and day. The standard wind product has 25 km spatial resolution. QuikSCAT provides significant improvement over ERS scatterometers in observing wind convergence; the scatterometers on ERS spacecraft cover only 41% of the global ocean daily, at 50 km spatial resolution. A review of space-borne scatterometers and the validations of their retrieved winds are given by *Liu* [2002]. Ocean surface winds from QuikSCAT are objectively interpolated [*Liu et al.*, 1998] to  $0.5^\circ$  latitude by  $0.5^\circ$  longitude grid and then averaged monthly.

[8] SST from Tropical Rain Measuring Mission Microwave Imager (TMI) [*Wentz et al.*, 2001b] were acquired as bin averages at  $0.25^\circ$  latitude by  $0.25^\circ$  longitude and daily resolution, separated according to ascending and descending orbits. The data were then averaged together to form monthly and  $0.5^\circ$  gridded fields, similar to the wind vectors from QuikSCAT.

[9] Data from July 1999 to March 2002 are used in this study. The strength of the equatorial upwelling that separates the double ITCZ is known to change with El Niño/Southern Oscillation (ENSO). A common indication of ENSO is the SST anomalies in  $5^\circ\text{N}$ – $5^\circ\text{S}$ ,  $90^\circ\text{W}$ – $150^\circ\text{W}$ , called Niño3. For 1999, the Niño3 index shows that SST in the equatorial eastern Pacific is more than  $1^\circ$  cooler than normal, indicating moderate La Niña conditions and favoring the establishment of double ITCZ. For most of 2000 and 2001, Niño3 is less than  $0.5^\circ$  below normal, indicating rather neutral ENSO conditions.

#### 4. Observations

[10] The surface wind convergence is defined as,  $C = -(\frac{\partial u}{\partial x} + \frac{\partial v}{\partial y})$ , where  $u$  and  $v$  are the zonal and meridional components of surface winds. The ITCZ north of the equator in both the Pacific and Atlantic oceans is clearly delineated by  $C$ , derived from QuikSCAT data in Figure 1. Wind convergence south of the equator is not confined to boreal spring in the eastern Pacific, and to boreal summer in the western Atlantic, as inferred in previous studies. Weaker convergence zones are also obvious south of the equator for all seasons, across the entire eastern Pacific and Atlantic. The major features are in good agreement with the climatological wind divergence maps compiled by *Hastenrath and Lamb* [1977] from ship reports; the almost year-round presence of wind convergence south of the equator in both the eastern Pacific and the Atlantic revealed by them has received little notice and discussion in the past.

[11] In the Atlantic, Figures 2a and 2b show that the northern ITCZ, denoted by high  $C$ , is collocated approximately with the  $v = 0$  line, where the northerly wind meets the southerly winds and  $v$  changes from positive to negative. This is also the location of the local maxima of SST, in general. In the eastern Atlantic (Figure 2a), a weaker ITCZ is present south of the equator, almost all year round, except for the September–October period. In the western Atlantic (Figure 2b), the ITCZ splits into north and south branches between May and December. The Atlantic, south of the northern ITCZ, is largely dominated by southerly winds, all year round. Because no northerly winds are observed blowing from the equator to the SITCZ, a mechanism different from the one described in section 2 is needed.

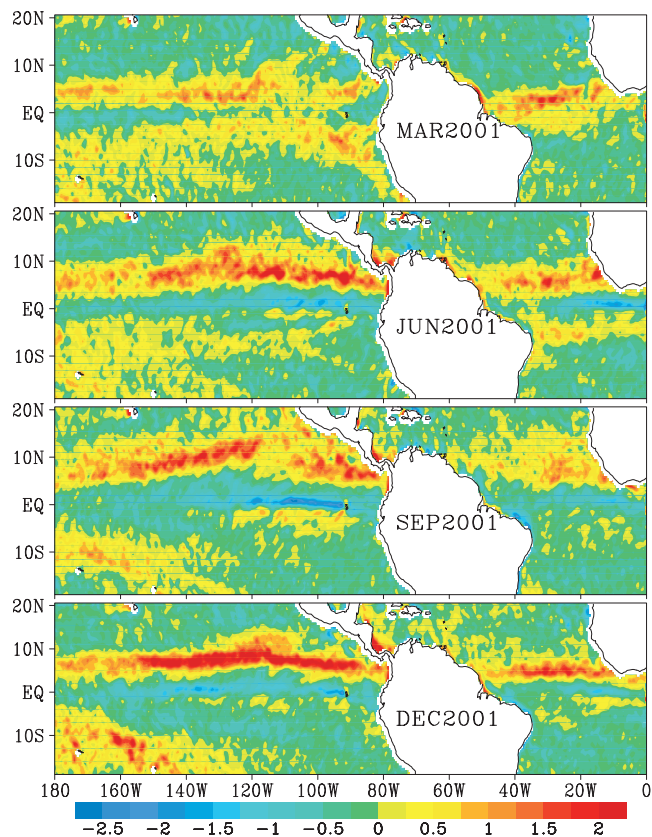


**Figure 1.** Surface wind convergence ( $10^{-5}/\text{s}$ ) from QuikSCAT for four typical months.

[12] The scenario is similar in the eastern Pacific (Figure 2c), except that, during boreal springs, the northerly trade winds cross the equator and meet the southerly trade winds at the stronger convergence south of the equator. They are consistent with the conceptual models of *Lietzke et al.* [2001] and *Halpern and Hung* [2001] for the SITCZ, except a different model is needed for the weaker ITCZ north of the equator, during this season. The stronger convergence zones are usually located where SST is above the generally accepted threshold for deep convection of  $27.5^\circ\text{C}$  [e.g., *Graham and Barnett*, 1987], except in the eastern Pacific during the 1999–2000 boreal winter when the ocean was exceptionally cool.

#### 5. Two Mechanisms

[13] Near the equator,  $-\partial u/\partial x$  is much smaller than  $-\partial v/\partial y$ ;  $C$  is dominated by the meridional gradient of the meridional wind component. There are two scenarios to achieve local maximum of  $C$ . High  $C$  occurs when  $v$  changes from positive to negative, where the southerly trade winds meet the northerly trade winds over the warm water. For the 32 months of QuikSCAT observations, this type of convergence took place only on one side of the equator, not on both sides. The coexistence of a stronger convergence zone on one side of the equator with a weaker one on the other side cannot be explained with the same mechanism. The second scenario is that local convergence occurs when  $v$  decelerates. As the trade winds move from the warmer water with a relatively well-mixed boundary layer towards

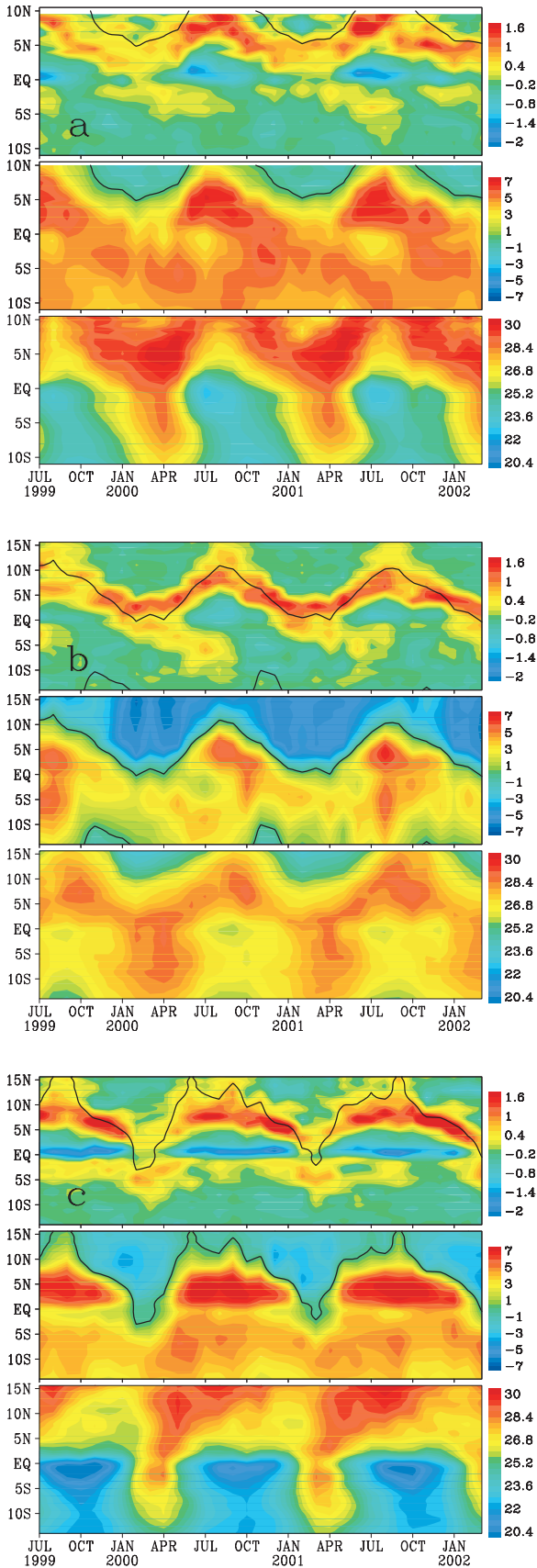


**Figure 2.** Latitude-time variations of (from top to bottom)  $C$  ( $10^{-5}/s$ ),  $v$  (m/s), and SST ( $^{\circ}C$ ), from QuikSCAT and TMI, averaged over (a)  $5^{\circ}W-15^{\circ}W$ , (b)  $25^{\circ}W-35^{\circ}W$ , and (c)  $95^{\circ}-105^{\circ}W$ . On the black line, the meridional wind is zero.

the cold upwelling water near the equator, vertical mixing is suppressed and wind shear increases. The trade winds decelerate and create a region of convergence just before they reach the cold water.

[14] The relation between wind shear and atmospheric density stratification (stability) has been well known, and discussed in turbulence transfer literatures. A review on atmospheric stability driven by wind shear and buoyancy is given by *Liu et al.* [1979] and others. At SST  $> 25^{\circ}C$ , *Liu* [1990] demonstrated that vertical moisture gradient exceeds temperature gradient in affecting stability. This model of tropical ocean atmosphere coupling through vertical mixing was postulated by *Wallace et al.* [1989] and was first used by *Xie et al.* [1998] to explain the coherence between SST and surface wind in the tropical instability waves (TIW) - the westward propagating temperature front of the cold tongue. *Liu et al.* [2000] validated this model with rawinsonde measurements of a research cruise across the TIW, and with the phase difference between the wind components measured by QuikSCAT and SST from TMI. The same model was implied in a number of studies of TIW, including *Wentz et al.* [2000] who tested the model with the boundary parameterization of *Liu et al.* [1979], and *Hashizume et al.* [2002] who related boundary layer structure to pressure gradient using rawinsonde soundings. The first scenario, which is consistent with pressure gradient hypothesis of *Lindzen and Nigam* [1987], appears to govern the strong convergence with deep convection, over warmer water. The second scenario appears to govern weaker convergence over cooler water.

[15] Figure 3a clearly shows that the meridional variation of  $C$  is dominated by  $-\partial v/\partial y$ ; both parameters are scaled by the same factor. The maximum value of  $C$  is found at  $8^{\circ}N$  where  $v$  changes from negative to positive over the local maximum of SST. This is consistent with the first scenario. South of this latitude,  $v$  is positive, indicating southerly winds over a wide span of ocean. A weaker convergence zone, with local maximum value of  $C$  and  $-\partial v/\partial y$ , is found at  $6^{\circ}S$ . This zone is located between the warmer water and higher wind speed to the south and the colder water and lower wind speed to the north. Here the southerly winds decelerate before they reach the cold water at the equator. The meridional profiles shown in Figure 3a are typical to the eastern Pacific and Atlantic for most of the year, when the northern convergence zone is stronger than the southern one. During boreal springs in the eastern Pacific, a north-south reversal is found, as shown in Figure 3b. The SST in the south is higher than that in the north, and the first scenario described above happens in the south. The northerly winds cross the equator and meet the southerly winds at  $3^{\circ}S$ . The northerly trades decelerate to form the convergence zone between  $2^{\circ}N$  and  $5^{\circ}N$ . The profiles are consistent with Figure 2.

## 6. Discussion

[16] Previous studies on the double ITCZ described only areas of strong surface wind convergence, which have clear manifestation in clouds and precipitation. The QuikSCAT winds reveal that the double ITCZ is much more extensive, with the weaker wind convergence found in the entire Atlantic and eastern Pacific, almost all year round. The strong ITCZ occurs when the northerly winds meet the

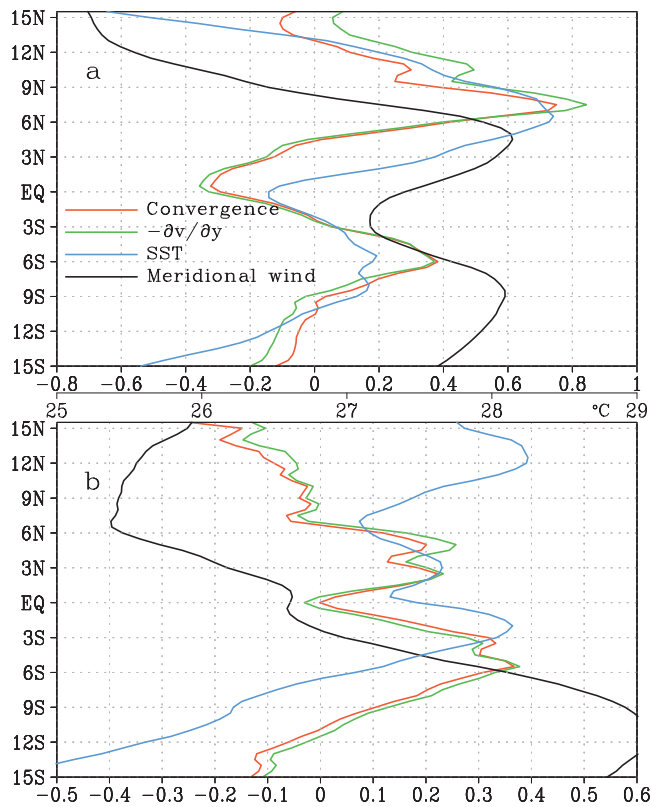


**Figure 3.** Meridional profiles of  $C$ ,  $-\partial v/\partial y$ ,  $v$ , and SST. The first two parameters are scaled by the same factor ( $2 \times 10^{-5}/s$ ) and the third by 7 m/s. The profiles are derived from QuikSCAT and TMI data, and averaged (a) between  $25^{\circ}W$  and  $35^{\circ}W$  for July 2000, and (b) between  $95^{\circ}W$  and  $105^{\circ}W$  for March 2000.

southerly winds over warm water, resulting in deep convection. The weaker ITCZ is caused by the deceleration of the surface winds as they approach the cold upwelling water near the equator.

[17] The QuikSCAT winds are limited to 32 months and are not sufficient to discern interannual variations. Although ocean wind vectors from the ERS scatterometers and from the Special Sensor Microwave Imager [Atlas *et al.*, 1996] do not have the spatial resolution to provide the quality of wind convergence as QuikSCAT, they provide longer time series of data - 1992–2001, and 1987–2001, respectively. New characteristics of  $v$  before July 1999 are revealed by the two sensors during boreal springs in the eastern Pacific. Unlike 2000–2002, the northeast trades did not cross the equator except in 1989. In 1994, 1996, and 1999, weak surface winds are found blowing both northward and southward from the equatorial cold water towards the double ITCZ.

[18] Associated with the weak SITCZ, QuikSCAT also reveals a zone of negative wind stress curl (WSC), which is hardly discernable in the operational wind products of numerical weather prediction such as those from European Center of Medium Range Weather Forecasts and the National Center of Environmental Prediction. The WSC induces upward Ekman pumping and Sverdrup transport in the ocean. The observed WSC by QuikSCAT, with magnitudes stronger than  $1.2 \times 10^{-7} N/m^3$ , would have signifi-

cant influence on wind-forced ocean currents [e.g., Kessler *et al.*, 2002].

[19] **Acknowledgments.** This study was performed at the Jet Propulsion Laboratory, California Institute of Technology, under contract with the National Aeronautics and Space Administration (NASA). It was supported jointly by the Physical Oceanography, the Ocean Vector Wind, and the TRMM programs of NASA.

## References

- Atlas, R., R. Hoffman, S. Bloom, J. Jusem, and J. Ardizzone, A Multi-year Global Surface Wind Velocity Data Set Using SSM/I Wind Observations, *Bull. Amer. Meteor. Soc.*, 77, 869–882, 1996.
- Graham, N. E., and T. P. Barnett, Sea surface temperature, surface wind divergence, and convection over tropical oceans, *Science*, 238, 657–659, 1987.
- Grodsky, S. A., and J. A. Carton, Relationship between the south trade winds convergence east of North-East Brazil and equatorial upwelling in the Atlantic Ocean, *Eos, Trans. of AGU*, 82, F628, (abstract), 2001.
- Halpern, D., and C.-W. Hung, Satellite observations of the southeast Pacific intertropical convergence zone during 1993–1998, *J. Geophys. Res.*, 106, 28,107–28,112, 2001.
- Hashizume, H., S.-P. Xie, M. Fujiwara, M. Shiotani, T. Watanabe, Y. Tanimoto, W. T. Liu, and K. Takeuchi, Direct observations of atmospheric boundary layer response to SST variations associated with tropical instability waves over the eastern equatorial Pacific, *J. Climate*, in press, 2002.
- Hastenrath, S., P. J. Lamb, *Climate Atlas of the Tropical Atlantic and Eastern Pacific Oceans*, Univ. of Wisconsin Press, 1977.
- Hubert, L. F., A. F. Krueger, and J. S. Winston, The double intertropical convergence zone - fact or friction?, *J. Atmos. Sci.*, 26, 771–773, 1969.
- Kessler, W. S., G. C. Johnson, and D. W. Moore, Sverdrup and nonlinear dynamics of the Pacific South Equatorial current, *J. Phys. Oceanogr.*, submitted, 2002.
- Lietzke, C. E., C. Deser, and T. H. Vonder Haar, Evolutionary structure of the eastern Pacific double ITCZ based on satellite moisture profile retrievals, *J. Climate*, 14, 743–751, 2001.
- Lindzen, R. S., and S. Nigam, On the role of sea-surface temperature gradients in forcing low-level winds and convergence in the tropics, *J. Atmos. Sci.*, 44, 2440–2458, 1987.
- Liu, W. T., Remote Sensing of surface turbulence flux, *Surface Waves and Fluxes*, Vol. II, edited by G. L. Geernaert and W. J. Plant, Kluwer Academic, Chapter 16, 293–309, 1990.
- Liu, W. T., Progress in scatterometer application, *J. Oceanogr.*, 58, 121–136, 2002.
- Liu, W. T., K. B. Katsaros, and J. A. Businger, Bulk parameterization of air-sea exchanges of heat and water vapor including the molecular constraints at the interface, *J. Atmos. Sci.*, 36, 1722–1735, 1979.
- Liu, W. T., W. Tang, and P. S. Polito, NASA Scatterometer provides global ocean-surface wind fields with more structures than numerical weather prediction, *Geophys. Res. Lett.*, 25, 761–764, 1998.
- Liu, W. T., X. Xie, P. S. Polito, S. Xie, and H. Hashizume, Atmosphere manifestation of tropical instability waves observed by QuikSCAT and Tropical Rain Measuring Missions, *Geophys. Res. Lett.*, 27, 2545–2548, 2000.
- Waliser, D. E., and C. Gautier, A satellite-derived climatology of the ITCZ, *J. Climate*, 6, 2162–2174, 1993.
- Wallace, J. M., T. P. Mitchell, and C. Deser, The influence of sea-surface temperature on surface wind in the eastern equatorial Pacific: Seasonal and interannual variability, *J. Climate*, 2, 1492–1499, 1989.
- Wentz, F. J., C. Gentemann, D. Smith, and D. Chelton, Satellite measurements of sea surface temperature through clouds, *Science*, 288, 847–850, 2000.
- Wentz, F. J., P. D. Ashcroft, and C. L. Gentemann, Post-launch calibration of the TMI microwave radiometer, *IEEE Trans. Geosci. and Remote Sensing*, 39(2), 415–422, 2001.
- Xie, S.-P., M. Ishiwatari, H. Hashizume, and K. Takeuchi, Coupled ocean-atmosphere waves on the equatorial front, *Geophys. Res. Lett.*, 25, 3863–3866, 1998.
- Zhang, C., Double ITCZ, *J. Geophys. Res.*, 106(11), 11,785–11,792, 2001.
- Zheng, Q., X.-H. Yan, W. T. Liu, and W. Tang, Seasonal and interannual variability of atmospheric convergence zones in the tropical Pacific observed with ERS-1 scatterometer, *Geophys. Res. Lett.*, 24, 261–263, 1997.